DESIGN, STRUCTURAL OPTIMIZATION AND LOADS ASSESSMENT FOR A FLYING WING

A. Voß, T. Klimmek and K. Bramsiepe, DLR - German Aerospace Center, Institute of Aeroelasticity
Busenstraße 10, 37073 Göttingen, Germany

Abstract

This paper presents a summary of the evolution of aeroelastic models for flying wing configurations. Two different flying wing configurations have been studied and synergies with other DLR projects have been used to validate important parts of the loads process. A newly developed in-house software for aircraft loads extends the aeroelastic design process in combination with a parametric model generation software and a structural optimization sequence. During the progress from the DLR-F19-S towards the MULDICON, the numerical methods evolved as well, mainly aiming for higher fidelity to ensure a thorough and sophisticated design. Design and loads related studies were performed with national and international partners from industry and academia. This paper gives an overview on aspect and modeling strategies that distinguish flying wings from classical wing-fuselage-empennage configurations. Finally, an outlook is given on the next steps and on ongoing work.

Keywords

Flying wing, aeroelasticity, maneuver, gust and landing loads, structural optimization, structural condensation

1. MOTIVATION AND INTRODUCTION

The design process for new aircraft configurations is complex, very costly and often takes several years until completion. The involved disciplines, like aerodynamics, structure, loads analysis, aeroelasticity, flight mechanics, and weights, define requirements, develop a first concept, conduct analyses, and carry out trade studies. All disciplines are equally important and have to interact. Thus, there is no clear beginning and dependencies are complex. At the end of the preliminary design phase, the aim is to substantiate the selected design, based on physically meaningful simulations and analyses. The more thorough the investigations and the better the methods, the more reliable is the preliminary design. In the detail design phase, modifications are much more costly and might lead to a delay of the design process and even a delay of the entry into service. Thus, the preliminary design should be as good as possible to avoid any “surprises” during a later stage. At the end of the detail design, the aircraft usually needs to be certified by an aviation authority, e.g. the European Aviation Safety Agency (EASA). Apart from other requirements, it has to be shown that the aircraft withstands the loads that are specified in the Certification Specifications, e.g. CS-23 [5] for small aircraft or CS-25 [4] for large aircraft, depending on the specifications that have to be applied.

Generally, flying wings are different from classical wing-fuselage-empennage configurations, and little knowledge and experience exists. Some unique characteristics of flying wings are:

- Compared to classical wing-fuselage-empennage configurations, flying wings require unconventional structural layouts. No typical and well-proven layouts exist.
- Because pitching stability is low, the gust encounter of flying wings requires a fully dynamic, unsteady simulation including flight mechanics.

doi:10.25967/480003

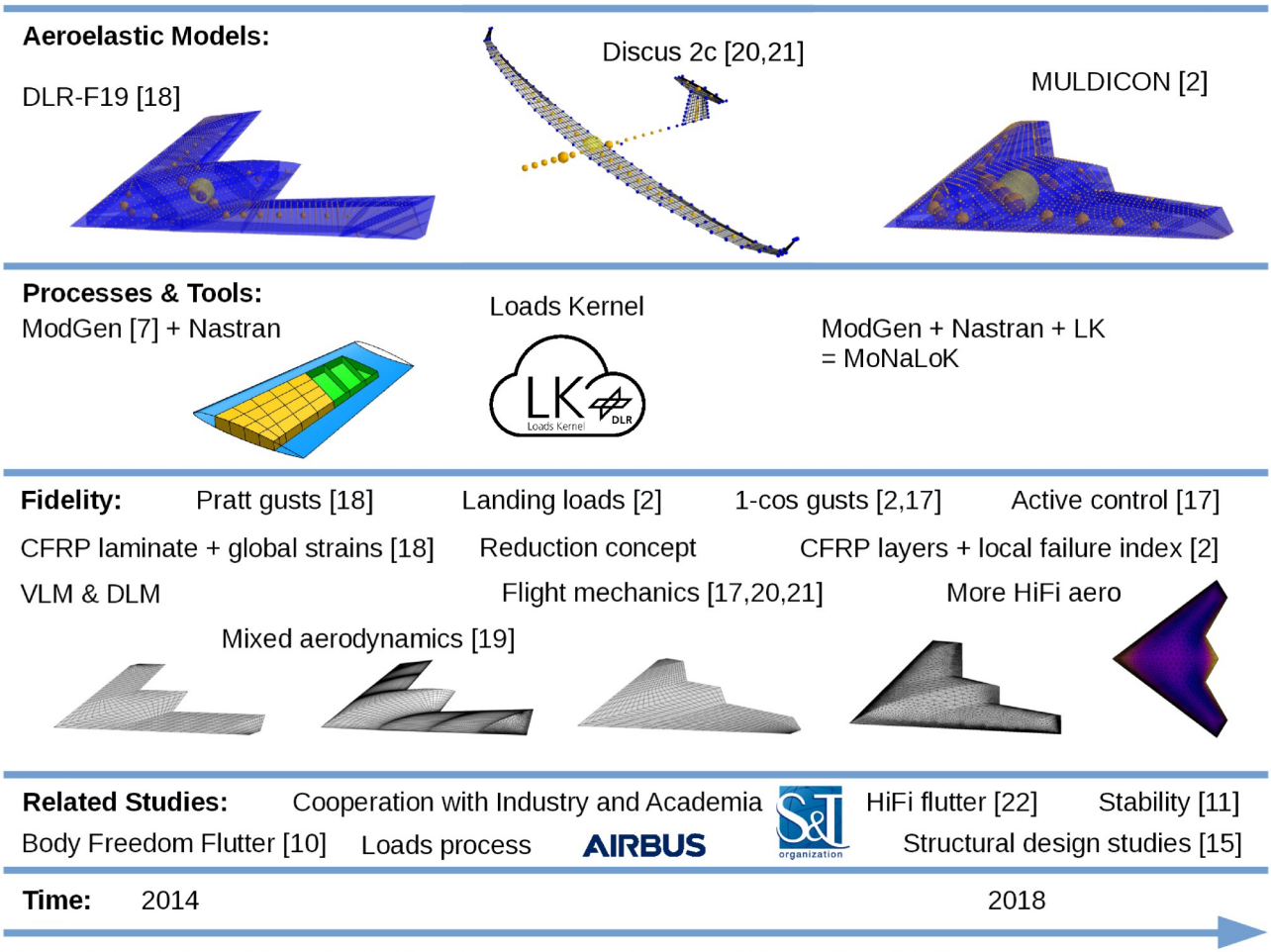

Figure 1: Evolution of Aeroelastic Models, Processes, Tools and Simulation Fidelity

- In case an active controller for the pitching motion is involved, it interacts with gusts. The combination of both increases the aircraft loads.
- Also, strong three-dimensional flow characteristics and transonic effects have an influence on the structural design and should be included in the preliminary design of flying wings.

The aim is to include these requirements in the preliminary design as early as possible. This is a trade off, because the corresponding analyses require a detailed knowledge of the structure, the mass distribution, the structural dynamic characteristics as well as the steady and unsteady aerodynamics, which become available only later during the design process. New methodologies for the design and optimization of a structural concept for an unconventional flying wing configuration have to be developed. The design needs to respect given specifications, e.g. geometry, aerodynamic profiles and available space for components and systems.

During the last years, this trade off led to the development of a comprehensive algorithmic design process that already allows the set-up of aeroelastic simulation models at an earlier stage of the design process. Parametric aeroelastic models are the state of the art and have been applied successfully to various conventional configurations and to some extend also to unconventional configurations.

This paper aims to summarize the design activities for flying wing configurations at the Institute of Aeroelasticity, starting in 2014 until today (2018). An overview is given in Figure 1.

Evolution of aeroelastic models: Two flying wing configurations have been developed, first for the DLR-F19-S and then for the MULDICON. Synergies with other project have been used to validate parts of the loads process at the example of the Discus 2c sailplane.

Evolution of Processes & Tools: The aeroelastic design process using the parametric model generation software ModGen in combination with Nastran is extended. The newly developed in-house software Loads Kernel replaces the previously used loads solution sequences of Nastran for more physical analyses.

Increased simulation fidelity: During the progress from the DLR-F19-S towards the MULDIOCN, also the numerical methods evolved, mainly aiming for higher fidelity to ensure a thorough and sophisticated design. Quasi-steady gust loads used for the sizing of the DLR-F19-S [18] have been replaced by fully dynamic, unsteady 1-cos gusts simulations [2,17]. Next to maneuver and gust loads, a generic landing gear module has been added to simulate loads from the landing impact in [2]. It includes the typically non-linear spring-damper-system of the landing gear and the interaction with the rigid and flexible aircraft motions. The influence of active control is investigated in [17]. Also, flight mechanical aspect are included [17], which could be validated against flight test data [20,21]. On the structural side, the carbon fiber reinforced plastic (CFRP) material is modeled in greater detail and uses more suitable material constraints [2]. A suitable concept for structural condensation has been prepared and is presented in this work in Section 4. On the aerodynamic side, studies have been performed to evaluated and to incorporate aerodynamics from higher fidelity methods [19]. Work to use even more high fidelity aerodynamics already in the preliminary design is ongoing. Summing up, the loads simulations for the MULDICON have been improved in many ways with respect to the DLR-F19-S.

Related studies: In all cases, the resulting aeroelastic models were subject to further flight physical studies. Schäfer et al. [10] shows Body Freedom Flutter (BFF) analyses based on the DLR-F19-S. The aeroelastic models are also used by G. Voss et al. [22] to perform flutter analyses using high fidelity aerodynamics. Stability analyses for the MULDICON are presented by Schreiber et al. [11]. Schweiger et al. [15] show a summary on design studies performed within the NATO Science and Technology community. In addition, the aeroelastic models were exchanged in a cooperation with Airbus D&S and loads related studies and comparisons were conducted. In all cases, very valuable feedback was obtained from the partners form industry and academia.

2. PARAMETRIC AEROELASTIC MODELING

The parametric modeling approach is a key concept of the aeroelastic design process. All involved simulations and optimization models are set up in a sequentially running process.

In the first step for each component (left and right wing, control surfaces) a geometry model of the outer geometry is defined by typical geometrical functions from Computer Aided Geometrical Design (CAGD) like B-splines for curves (e.g. aerodynamic profiles) and surfaces (outer geometry). Then the load carrying structural parts like spars, ribs and skin are set up as well with geometrical functions, while their number, position, and orientation follows a previously defined construction rules. Such parameterized process uses common intersection, approximation, and interpolation methods from CAGD and ensures reasonable and practical structural models of the load carrying structure. For the meshing of the finite element model the geometrical surfaces, that result from intersection among each other, are used (e.g. ribs are subdivided by spars or the skin surface is subdivided by spars and ribs). They are called sub-surfaces.

Besides the finite element model (nodes and elements) all other simulation models and the optimization model of the structural optimization are created after the geometrical model and the finite element model have been set up. This comprises the aerodynamic model for the DLM as well as elements to attach mass items to the load carrying structure e.g. for the engine, landing gear, fuel mass items, and various other system items. For the optimization model the design variables like the thickness of a structural sub-surface are defined. Herein the elements of one sub-surface constitute one design field. For the constraints, structural responses like stress, strain, and structural failure for all elements that are part of the design variable model, are created for MSC Nastran SOL200. The geometry model of the structural layout is also used to define fuel tanks and fuel levels in order to generate concentrated mass items representing

various fuel configurations. For all “models” involved see Figure 2.

For the automatized set-up the all simulation models where the described model set-up concept is implemented, the computer program ModGen was developed at DLR. Compared to its capabilities outlined in [7], some further developments could be achieved over time. They are outlined as follows.

For typical transport aircraft, only the wing box is taken into account for the structural model of the load carrying structure. For flying wing configurations, the leading and trailing edge areas have to be included for the structural models. Therefore essentially fictitious spars at the leading and at the trailing edge are defined to create corresponding sub-surfaces of the spars, ribs, and skins for leading and trailing edge structural modeling.

As openings and cut outs of the structure are more relevant for flying wing configurations, the option not to mesh selected sub-surface, like the landing gear or the payload doors, was used. Therewith the weakened load carrying structure could be investigated.

As both the DLR-F19-S and the MULDICON are designed with carbon fiber material, the parametric modeling process was also enhanced to deal with such material for the structural analysis and the structural optimization (e.g. definition of design variables and constraints).

Regarding the aerodynamic model, a parametric surface for the complete planform representing the camber characteristic of the profiles is created within the design process. That surface is used to estimate the local angle of attack of each aerodynamic box of the VLM / DLM (see Figure 3). For the consideration of the camber within the loads analysis the so-called W2GJ matrix, following MSC Nastran conventions, is used.

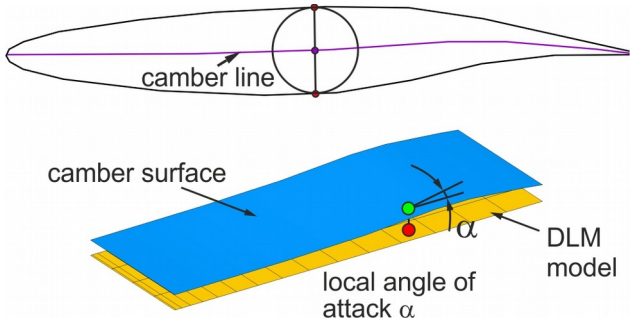

Figure 3: Camber characteristic estimated at the profile and transferred to the VLM / DLM model

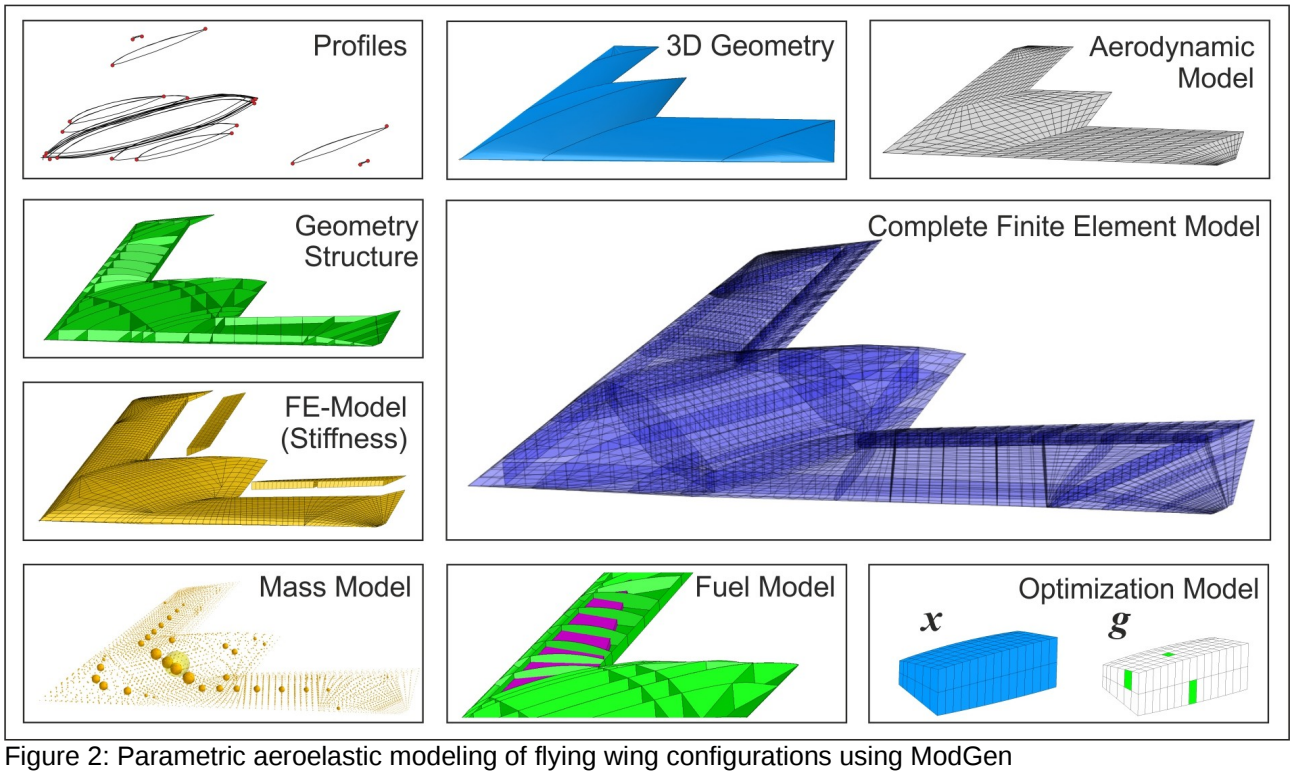

Figure 2: Parametric aeroelastic modeling of flying wing configurations using ModGen

3. MODEL SET-UP OF THE DLR-F19-S

This section summarizes the set-up of the aeroelastic models for the DLR-F19-S. More details are found in [18].

3.1. Structural Model

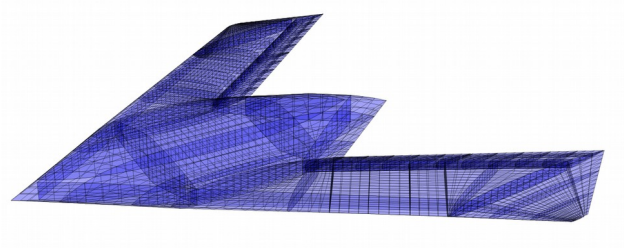

Figure 4: DLR-F19-S FEM

The focus on aeroelastic aspects leads to a number of requirements which differ from a classical finite element model for stress analysis. The structure should be as realistic as possible because global elastic characteristics such as wing bending and twist are of major interest. Local effects, like stress concentrations at sharp edges or at holes are neglected. This means that all primary structural components, such as spars, ribs, stringers and skin, should be modeled.

The structural model is set-up using the parametric modeling approach described in Section 2. The resulting finite elements (FE) model consists mainly of shell elements. A right-hand side and a corresponding symmetric left-hand side FE model are joined at the center line through RBE2 elements. The spars, ribs and skins are modeled as shell elements and are equipped with stiffening elements to keep the buckling fields sufficiently small and reduce local eigenmodes. For the stringers, a hat profile is selected. The control surfaces are structurally modeled as well and attached to the wing elastically.

For all structural components, suitable carbon fiber composite properties are chosen (details given in Table 1 in [18]). For the skin, the 0° plies are aligned along the leading edge using a local coordinate system to define the orientation. Material properties for unidirectional layers are provided by the DLR Institute of Composite Structures and Adaptive Systems. The material properties of the complete laminate setup are then calculated as described in [12]. The approach is based on the classical laminate theory (CLT) and on the calculation of stiffness matrices A and D of the complete laminate set-up.

3.2. Mass Model

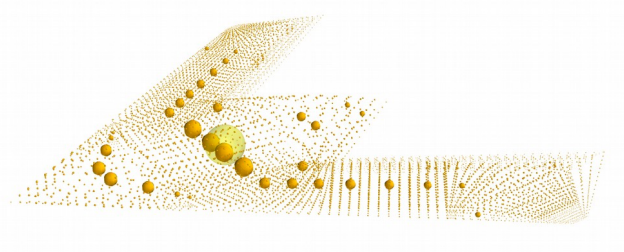

Figure 5: DLR-F19-S mass discretization for basic flight design mass (BFDM)

In addition to the structural stiffness aspects, a mass model with properly distributed mass entities (e.g., structure, systems, payload, fuel) and the consideration of various mass configurations (e.g., fuel, payload) are important to conduct dynamic calculations. The dynamic analysis of the stiffness and mass model should result in almost only global modes for a specified frequency range. Local modes are to be avoided. Because this is rarely possible, condensation strategies are required. A suitable concept is presented in Section 4.

3.3. Aerodynamic Models

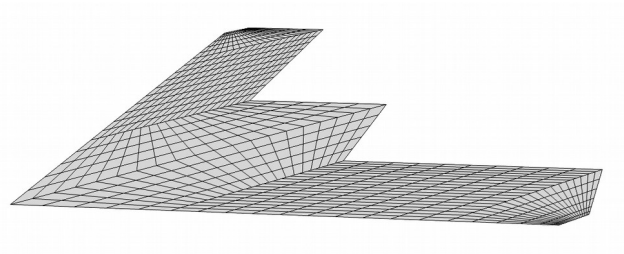

Figure 6: DLR-F19-S aerodynamic mesh for VLM & DLM

The underlying aerodynamic theories are the quasi-steady Vortex Lattice Method (VLM) and the unsteady Doublet Lattice Method (DLM). Both require a planar aerodynamic mesh as shown in Figure 6. The challenge for flying wings of low aspect ratio is to find a compromise between the rather long wing root and the short wing tip. At the same time, the aspect ratio of the panels needs to be lower than four and large jumps in the discretization should be avoided. Four control surfaces along the trailing edge need to be incorporated as well. To avoid any numerical issues due to triangular panels, the pointed wing tip is cut of for the VLM & DLM mesh.

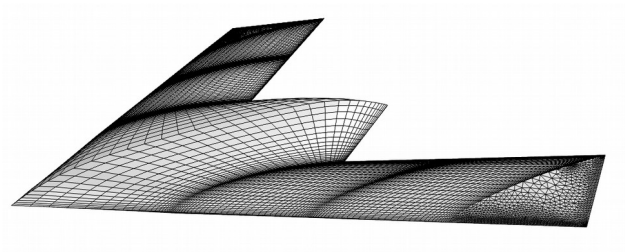

Figure 7: DLR-F19-S aerodynamic mesh for CFD

From the parametric modeling process described in Section 2, an outer surface geometry can be derived. That surface geometry is then easily meshed using a CFD meshing software such as Centaur. The undeformed CFD surface mesh is shown in Figure 7. The beauty of this approach is that the CFD mesh perfectly matches e.g. the underlying structural model. More information on the mesh properties and the related simulations are presented in [19]. To account for structural deformation and control surface deflections, the mesh is deformed geometrically using splining techniques presented in the next Section.

3.4. Coupling Model

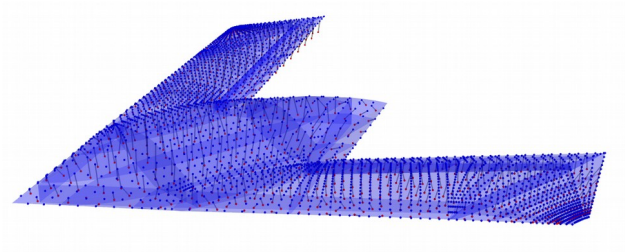

Figure 8: DLR-F19-S aero-structural coupling

In every numerical, aeroelastic application, forces need to be transferred onto the structure and deformations onto the aerodynamic mesh. Formally, the coupling (or splining) can be handled using a transformation matrix $\mathbf{T}_{di}$. Various splining techniques are available to construct that matrix.

The rigid body spline allows for a clear and comprehensible mapping of the aerodynamic grid to the structure. It is visualized by the small black lines in Figure 8. Due to the direct mapping of the rigid body spline, matrix $\mathbf{T}_{di}$ is sparse while $\mathbf{T}_{di}$ is dense when using a global surface or volume spline. To construct a surface or volume spline, a system of equations needs to be solved. This results in longer computational time in comparison to the rigid body spline. Although globally correct, a surface or volume spline may locally result in very large, opposing forces, which are not physical. This behavior has been observed when the number of structural grid points is much larger than the number of aerodynamic grid points. These large, local forces may change the magnitude of section loads significantly while the integral forces of the complete aircraft are correct. Therefore, the rigid body spline is more suitable for the transfer of forces and moments. In contrast, a surface spline is more suitable for smooth surface deformations while a rigid body spline usually results in bad and bumpy surface deformations. This is acceptable when using aerodynamic panel methods such as VLM or DLM, but may have a fatal impact on CFD simulations. A further discussion and a tabular overview is given in [19].

3.5. Optimization Model

The design objective for structural optimization is minimum structural weight. The design variable is the skin thickness of every design field, with one design field being the area between two ribs and spars. The constraints are the allowable strains of the material. The optimization problem for the DLR-F19-S has 168 design fields and 6926 design responses. As a side constraint, a minimum and maximum skin thickness $x_{lower} \leq x \leq x_{upper}$ is imposed.

Load cases from both maneuver and gust encounter are considered for the DLR-F19-S. They are down-selected based on section load envelopes (typically F_z, M_x, M_y) at monitoring stations. The selection process typically results in 50 to 60 dimensioning load cases.

For the MULDICON, the more detailed modeling of the carbon fiber material substantially increases the number of design responses. More details on the selection of the constraints is given in Section 6. The load cases are enhanced by fully dynamic and unsteady 1-cos gust simulations and dynamic landing loads.

4. MODEL REDUCTION STRATEGY FOR PLANAR AIRCRAFT

The degrees of freedom for a grid point of a finite element model includes the six components of displacement: translation in x, y, and z direction and rotation about the x, y, and z axis. In MSC.Nastran,

these degrees of freedom are organized in sets [23]. The relation of the most relevant sets for this work are shown in Figure 9. The global set, or g-set, contains all degrees of freedom and is the top-level set. Usually, the g-set contains linear relationships, for example constructed with the RBE and MPC cards. These dependent degrees of freedom are moved into the m-set. The remaining, independent degrees of freedom form the n-set. Sometimes, a structural model contains single point constraints, constructed with the SPC card, for example to realize a clamping. These degrees of freedom are moved into the s-set. The remaining degrees of freedom are organized in the f-set. Therefore, the f-set contains all “free” degrees of freedom, the corresponding matrices mass and stiffness matrices K and M are no longer singular and suitable for a solution if arranged in a set of equations.

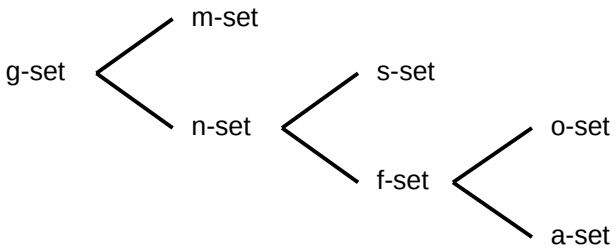

Figure 9: Schematic overview of structural sets

Finally, the f-set may be partitioned into the a-set and the o-set. This process is called static condensation or Guyan reduction. In aeroelastic applications, the wing and fuselage structure is often condensed to a loads reference axis (LRA). The loads reference axis is placed e.g. along the quarter chord line of the wing. A typical example is shown in Figure 10. Note that the points of the leading and trailing edge (LE and TE, green points) are connected with rigid body elements to the loads reference axis. The concept of a loads reference axis has several advantages. First, the model is simplified significantly, making physical interpretations more easy. In addition, mass estimates are often done by a different department than the structural analysis. The loads reference axis is a suitable basis for communication and data exchange, as condensed masses can be easily attached to the condensed structural grid points. Second, computational time is reduced for all following calculations. Depending on the number of load cases to be considered, this argument is still relevant as of today. Finally, local modes are avoided during the modal analysis. Such local modes appear if for example a thin shell element vibrates at a low frequency. Using a condensation, the model is “cleaned” from such local modes.

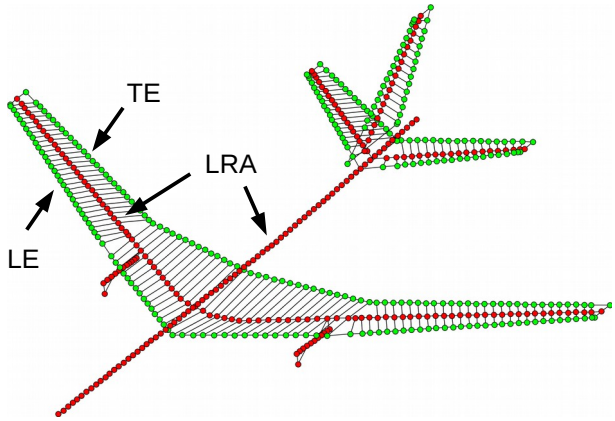

Figure 10: Condensed finite element model of the FERMAT configuration [8]

The equation for static deflection

(1) $$\mathbf{K} \cdot \mathbf{u} = \mathbf{p}$$

relating forces $\mathbf{p}$ to stiffness matrix $\mathbf{K}$ times deflections $\mathbf{u}$ can be rearranged to the following form according to Guyan [6]

(2) $$\begin{bmatrix} \mathbf{K}_{aa} & \mathbf{K}_{ao} \\ \mathbf{K}_{oa} & \mathbf{K}_{oo} \end{bmatrix} \cdot \begin{pmatrix} \mathbf{u}_a \\ \mathbf{u}_o \end{pmatrix} = \begin{pmatrix} \mathbf{p}_a \\ \mathbf{p}_o \end{pmatrix}.$$

Here, the degrees of freedom with index 'o' are those to which no force is applied to and which can be eliminated. With $\mathbf{p}_0 = 0$, the equations are solved to

(3) $$\left[\mathbf{K}_{aa} - \mathbf{K}_{ao} \cdot \mathbf{K}_{oo}^{-}1 \cdot \mathbf{K}_{oa}\right] \cdot (\mathbf{u}_a) = (\mathbf{p}_a).$$

From this, the reduced stiffness matrix $\mathbf{K}_{aa,reduced}$ is identified as

(4) $$\mathbf{K}_{aa,reduced} = \mathbf{K}_{aa} - \mathbf{K}_{ao} \cdot \mathbf{K}_{oo}^{-1} \cdot \mathbf{K}_{oa}.$$

Due to the analytical solution of the problem, the Guyan reduction of the stiffness matrix is exact.

The same procedure could be applied to the mass matrix $\mathbf{M}$, however, term $\mathbf{M}_{ao}$ is usually zero as mass matrices are usually diagonal. Multiplication with $\mathbf{M}_{ao}$ would eliminate all masses of the o-set and only the masses on the a-set would remain. This problem is solved by Guyan by combining mass and stiffness matrices as follows to obtain a reduces mass matrix, too.

$$\begin{aligned}\mathbf{M}_{aa,red} =& \mathbf{M}_{aa} - \mathbf{M}_{ao} \cdot \mathbf{K}_{oo}^{-1} \cdot \mathbf{K}_{oa} \\ & - (\mathbf{K}_{oo}^{-1} \cdot \mathbf{K}_{oa})^T \cdot (\mathbf{M}_{oa} \\ & - \mathbf{M}_{oo} \cdot \mathbf{K}_{oo}^{-1} \cdot \mathbf{K}_{oa})\end{aligned} \tag{5}$$

The influence of the masses on the o-set is weighted with the stiffness. Guyan states that “the eigenvalue-eigenvector problem is closely but not exactly preserved” [6]. Comparison studies show that this is true for low frequencies. The higher the frequency, the greater the deviation. However, for use with a typical aircraft configuration, the Guyan reduction is suitable.

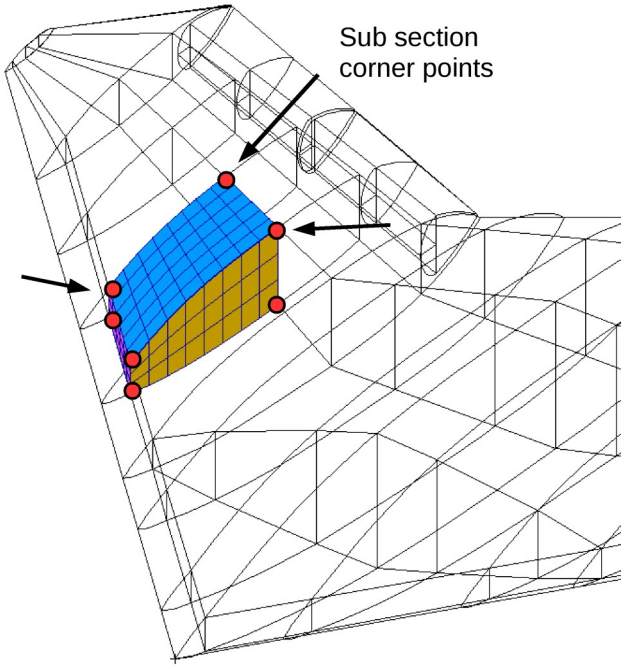

Figure 11: Selection of degrees of freedom of the a-set based of sub section corner points

Unfortunately, using a loads reference axis is very unsuitable for compact, planar flying wing configurations of low aspect ratio. There are only very few ribs in span wise direction and the fuselage bending characteristics would be neglected completely. A new condensation concept needs to be developed, which is based on sub-section corner points (SSCP). One sub-section is defined by two ribs and two spars, leading to eight corner points as sketched in Figure 11. Using this procedure, structurally important and spatial distributed points are identified all over the aircraft. This leads to an a-set with 1068 degrees of freedom (178 grid points) and a remaining o-set with 32636 degrees of freedom.

5. LOADS ANALYSIS

The aircraft structure is optimized based on loads from

- maneuver (306 load cases),
- gust (336 load cases) and
- landing impact (12 load cases).

The loads are primarily responsible for the weight of the load carrying structure. Also, emphasis is put on a comprehensive loads process including a large number of load cases (>100) to ensure a thorough preliminary design.

With a gust from below, the naturally stable classical wing-fuselage-empennage configuration typically performs a heave and nose down recovery motion and “dives” into the gust. Unsteady aerodynamics typically delay and reduce the impact of the gust (compared to quasi-steady aerodynamics, without aero-structural coupling).

Flying wings are different in several aspects. They are sensitive about pitch axis and large rigid body motions are expected. The MULDICON for example is only marginally stable, the empennage is missing, and the range of travel of the neutral point is large compared to the aircraft length. Due to the geometrical shape, the moment of inertia about pitch axis is low. Generally, penetration effects are pronounced with planar configurations where large areas of lifting surface is in front of the center of gravity. For the MULDICON, there is possibly a need for an active pitch control and unstable configurations are possible or even unavoidable. This requires fully dynamic, unsteady simulations of the gust encounter in the time domain, including flight mechanical aspects. More details on gust loads of flying wings are given in [17].

Dynamic landing impact simulations have been performed for 12 landing scenarios with mass configurations and sink speeds as requested by CS-25. The modeling of the landing gear is described in [2]. The loads envelopes of shear force F_z, bending moment M_x and torsion moment M_y at the right wing root show clearly that the landing loads are well within the envelopes of maneuver and gust, see Figure 12. In general, the landing loads were found to have little impact on the global aircraft

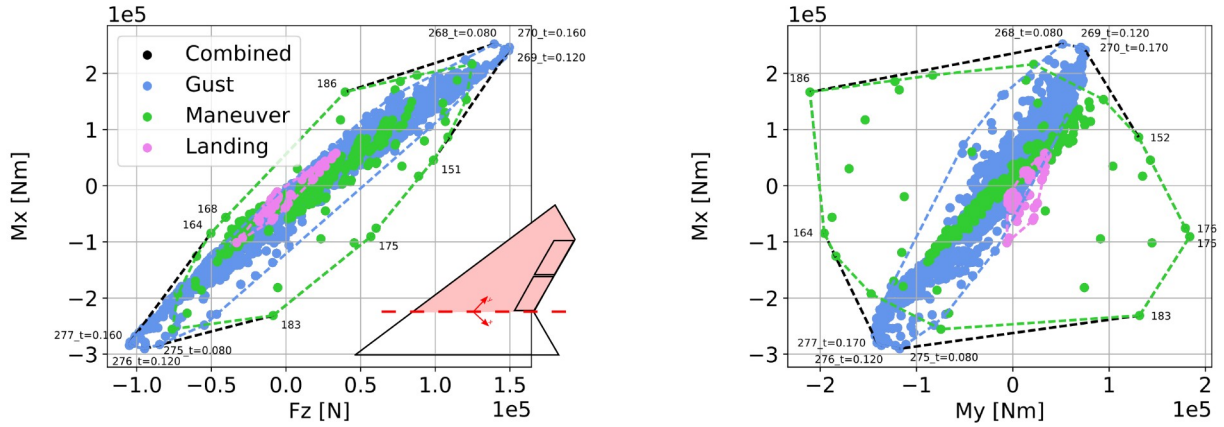

Figure 12: Loads envelope of shear force F_z, bending moment M_x and torsion moment M_y at the right wing root

structure and will presumably only lead to local reinforcements of the landing gear attachment structure.

While gust loads are dominated by unsteady aerodynamic and structural dynamic aspects, for maneuver loads steady aerodynamics are assumed to be more important. Therefore, the aim is to include more and more high fidelity aerodynamic methods in the preliminary design. Work concerning the inclusion of CFD in the optimization loop is currently ongoing.

6. ADVANCEMENTS OF MODELS

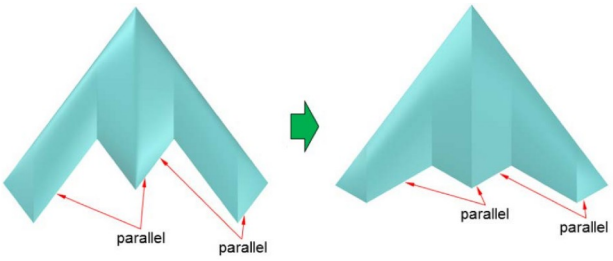

Figure 13: Moving towards MULDICON [14]

The MULDICON is also a flying wing configuration and the result of an evolution of the DLR-F19. Its wingspan is equal to the DLR-F19 wingspan of 15.375 m and the wing area is still 77.8 m². The new design is characterized by moving the trailing edge in rearward direction (see Figure 13). This was done to increase the effectiveness of the control surfaces [14]. Moreover, new airfoils are selected to improve flight characteristics [13]. Looking at the modeling side, these modification might have been accomplished by exploiting the parametric modeling approach. However, it was decided to take the opportunity to refine the aeroelastic modeling, leading to the set-up of a new structural model for the MULDICON. Special emphasis has been placed on the modeling of composite materials.

Instead of describing the stiffness of the laminate with the stiffness matrices A and D (PSHELL/MAT2) the model is now set up with a stiffness description of each ply (PCOMP/MAT8). This way yields the same stiffness matrices, the same deformations, and the same strains but enables for the analysis of each ply with a 'local' failure criterion. The analysis of every ply is necessary in an aircraft certification process due to the first ply failure approach. The VDI (Association of German Engineers) provides such a guideline for calculating composite laminates [16]. The four different ‘local’ failure criteria implemented in MSC Nastran have been studied and as a result the HILL criterion is selected for the structural optimization, because of its simplicity and conservatism.

The optimization is still done by a continuous increase of the laminate thickness and an unchanged stacking sequence. The chosen design fields and stiffnesses for skin, ribs, and spars are shown in Figure 14 and Figure 15. The optimization problem has 115 design variables with a failure criterion as constraints for each ply of each element as well as the minimum thickness for each field, leading to a total of 107275 constraints (DLR-F19-S: 168 design fields, 6926 constraints). The resulting model is sized with 654 load cases, including maneuver, gust, and landing loads. More details of the aeroelastic models and the resulting structure of the MULDICON are given in [2].

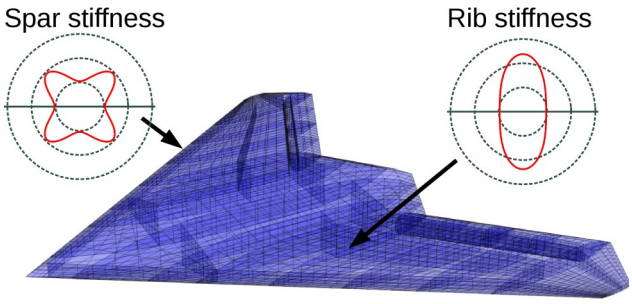

Figure 14: MULDICON FEM with the stiffness plots for spars and ribs

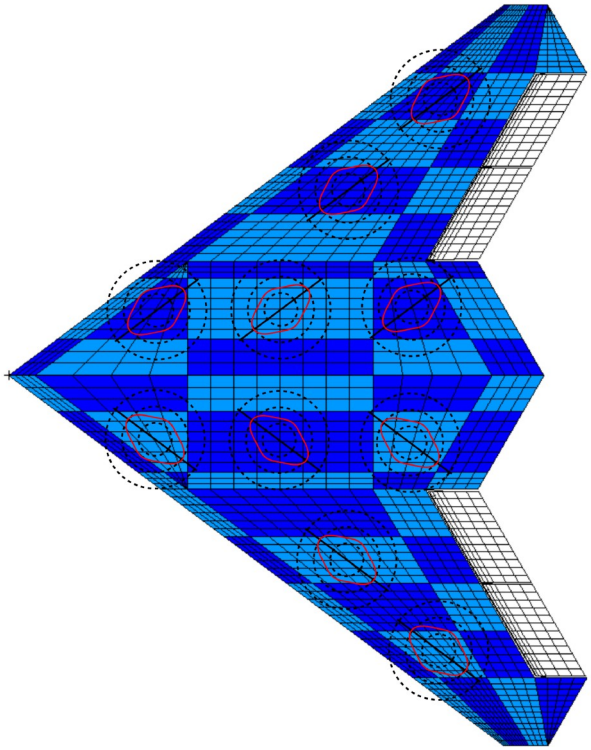

Figure 15: Top view of the MULDICON FEM with design fields and skin stiffness plots

Figure 16 shows three different failure criteria for plane stress in the corresponding strain space. The maximum strain criterion (black) is valid for its specific [0°, ±45°, 90°]s-laminate and describes the edges of the failure envelope with allowable strains. It is independent of the ply angles and thus a global failure criterion. The Tsai-Wu criterion (green) defines the envelope for a ply, depending on the allowable stresses of a unidirectional ply. The 'local' failure envelope can than be transformed to a 'global' failure envelope by the transformation matrix

$$\begin{bmatrix} \epsilon_x \\ \epsilon_y \\ \epsilon_{xy} \end{bmatrix} = \begin{bmatrix} c^2 & s^2 & -2sc \\ s^2 & c^2 & 2sc \\ sc & -sc & c^2 - s^2 \end{bmatrix} \cdot \begin{bmatrix} \epsilon_1 \\ \epsilon_2 \\ \epsilon_{12} \end{bmatrix} \quad (6)$$

with $c = cos(\theta)$ and $s = sin(\theta)$.

In comparison to the Tsai-Wu criterion (green), the Hill-criterion (red) utilizes also the allowable stresses, but stays inside the boundaries of the maximum stresses. Therefore, the Hill-criterion is conservative and also independent of a additional fiber fracture criterion, which is necessary for the Tsai-Wu criterion. For a [0°, ±45°, 90°]s-laminate the 'global' feasible regions of the two ply-dependent criteria are close to the feasible region of the maximum strain criterion because the matrix tension perpendicular to the fiber in a 90°-ply limits the tension in x-direction of the laminate and the fiber compression of a 0°-ply limits the compression in x-direction of the laminate.

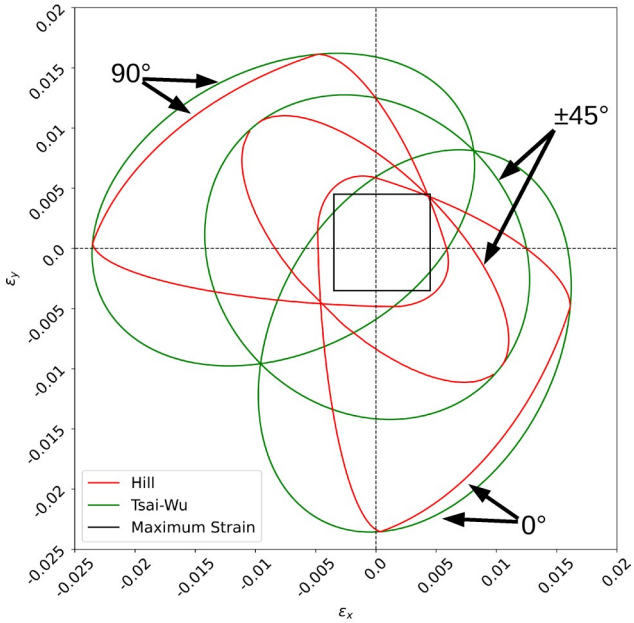

Figure 16: Failure envelopes for 0°, ±45°, and 90° of the Tsai-Wu criterion (green), the Hill criterion (red), and the maximum strain criterion (black) at ε_{xy}=0

7. SUMMARY AND OUTLOOK

Structural designs for two different flying wing configurations have been developed and optimized for minimum structural weight. State of the art parametric aeroelastic modeling techniques are extended and applied to these unconventional configurations. The aeroelastic design process in combination with a parametric model generation software (ModGen) and a structural optimization sequence (Nastran) is extended by a newly developed in-house software for aircraft loads (Loads Kernel). This allowed significant

improvements of the underlying numerical methods. During the progress from the DLR-F19-S towards the MULDIOCN, one focus was put on higher fidelity to ensure a thorough and sophisticated design. Fully dynamic 1-cos gusts and landing loads were included.

The unique characteristics of flying wings require special treatment during the loads analysis. Because pitching stability is low, the gust encounter of flying wings requires a fully dynamic, unsteady simulation including flight mechanics. In case an active controller for the pitching motion is involved, it interacts with gusts. It is shown that the combination of both decreases shear force and bending moment but increases the torsion moment at the wing root.

Also, strong three-dimensional flow characteristics and transonic effects have an influence on the structural design and should be included in the preliminary design of flying wings as early as possible.

Finally, a close collaboration with national and international partners from industry and academia, helped to establish a sophisticated design.

For a more detailed design, cut outs for the payload and landing gear bays could be included. Presumably, they will decrease the load carrying cross section and weaken the structural design. First studies showed no increase in structural weight but a substantial reduction of the aircraft's eigenfrequencies. At the same time, a variable stiffness for each design field could be used to fit the structure better to its loading. The currently favored procedure is based on a lamination parameters approach as explained in [1,3]. The continuous optimization of the lamination parameters is followed by a stacking sequence optimization with a generic algorithm, as presented in [9].

Next to its mass, the engine is suspected to have high inertia properties, which are currently not included. Also, a detailed knowledge of the engine attachment structure would improve the design. However, as mentioned in the introduction, this is a trade off, because detailed knowledge becomes available only later during the design process.

Finally, it was found difficult to select dimensioning load cases based of section loads at monitoring stations, especially in the fuselage region where the structure is over-determined and the load paths are not clear. An alternative concept remains to be investigated.

REFERENCES

[1] Bramsiepe, K., Handojo, V., Meddaikar, Y. M., Schulze, M., and Klimmek, T., “Loads and Structural Optimisation Process for Composite Long Range Transport Aircraft Configuration,” presented at the AIAA Aviation and Aeronautics Forum and Exposition, Atlanta, Georgia, 2018.

[2] Bramsiepe, K., Voß, A., and Klimmek, T., “Design and Sizing of an Aeroelastic Composite Model for An UCAV Configuration with Maneuver, Gust and Landing Loads,” presented at the Deutscher Luft- und Raumfahrtkongress, München, 2017.

[3] Dillinger, J. K. S., “Static aeroelastic optimization of composite wings with variable stiffness laminates,” Dissertation, TU Delft, 2014.

[4] European Aviation Safety Agency, ed., *Certification Specifications for Large Aeroplanes CS-25*. 2015.

[5] European Aviation Safety Agency, ed., *Certification Specifications for Normal, Utility, Aerobatic, and Commuter Category Aeroplanes CS-23*. 2012.

[6] Guyan, R., “Reduction of Stiffness and Mass Matrices,” *AIAA Journal*, vol. 3, no. 2, p. 280, 1964.

[7] Klimmek, T., “Parameterization of topology and geometry for the multidisciplinary optimization of wing structures,” in *CEAS 2009 - European Air and Space Conference*, Manchester, United Kingdom, 2009.

[8] Klimmek, T., “Parametric Set-Up of a Structural Model for FERMAT Configuration for Aeroelastic and Loads Analysis,” *Journal of Aeroelasticity and Structural Dynamics*, no. 2, pp. 31–49, May 2014.

[9] Meddaikar, Y. M., Irisarri, F.-X., and Abdalla, M. M., “Blended Composite Optimization combining Stacking Sequence Tables and a Modified Shepard’s Method,” presented at the 11th World Conference on Structural and Multidisciplinary Optimization, Sydney, Australia, 2015.

[10] Schäfer, D., Vidy, C., Mack, C., and Arnold, J., “Assesment of Body-Freedom Flutter for an Unmanned Aerial Vehicle,” presented at the Deutscher Luft- und Raumfahrtkongress, Braunschweig, 2016.

[11] Schreiber, P., Vidy, C., Voß, A., Arnold, J., and

Mack, C., “Dynamic Aeroelastic Stability Analyses of Parameterized Flying Wing Configurations,” presented at the Deutscher Luft- und Raumfahrtkongress, Friedrichshafen, 2018.

[12] Schürmann, H., *Konstruieren mit Faser-Kunststoff-Verbunden*. Berlin; Heidelberg; New York: Springer, 2007.

[13] Schütte, A., “Numerical Investigations of Vortical Flow on Swept Wings with Round Leading Edges,” *Journal of Aircraft*, vol. 54, no. 2, pp. 572–601, Mar. 2017.

[14] Schütte, A., Huber, K. C., and Zimper, D., “Numerische aerodynamische Analyse und Bewertung einer agilen und hoch gepfeilten Flugzeugkonfiguration,” presented at the Deutscher Luft- und Raumfahrtkongress, Rostock, 2015.

[15] Schweiger, J., Cunningham, A., Sakarya, E., Dalenbring, M., and Voß, A., “Structural Design Efforts for the MULDICON Configuration,” presented at the AIAA AVIATION Forum, Atlanta, Georgia, 2018.

[16] VDI-Fachbereich Kunststofftechnik, “Entwicklung von Bauteilen aus Faser-Kunststoff-Verbund - Berechnungen,” Verein Deutscher Ingenieure, Richtlinie VDI 2014 Blatt 3, Sep. 2006.

[17] Voß, A., “Gust Loads Calculation for a Flying Wing Configuration,” presented at the AIAA AVIATION Forum, Atlanta, Georgia, 2018.

[18] Voß, A., and Klimmek, T., “Design and sizing of a parametric structural model for a UCAV configuration for loads and aeroelastic analysis,” *CEAS Aeronautical Journal*, vol. 8, no. 1, pp. 67–77, Mar. 2017.

[19] Voß, A., and Klimmek, T., “Maneuver Loads Calculation with Enhanced Aerodynamics for a UCAV Configuration,” presented at the AIAA AVIATION Forum, Washington, D.C., 2016.

[20] Voß, A., and Ohme, P., “Dynamic maneuver loads calculations for a sailplane and comparison with flight test,” *CEAS Aeronautical Journal*, pp. 1–16, Apr. 2018.

[21] Voß, A., Pinho Chiozzotto, G., and Ohme, P., “Dynamic Maneuver Loads Calculation for a Sailplane and Comparison with Flight Test,” presented at the IFASD 2017 - 17th International Forum on Aeroelasticity and Structural Dynamics, Como, Italy, 2017.

[22] Voss, G., Schäfer, D., and Vidy, C., “Investigations on flutter stability of the DLR-F19/Saccon configuration,” presented at the AIAA Aviation, Atlanta, Georgia, 2018.

[23] *MSC.Nastran 2005 Quick Reference Guide*. MSC Software Corporation, 2004.